3-D General Relativistic MHD Simulations of Generating Jets

Ken Nishikawa (*Rutgers University*)

S. Koide (*Toyama University*)

K. Shibata (*Kyoto University*)

T. Kudoh (*NAO, Mitaka*)

H. Sol (*Obs. de Paris-Meudon*)

J. Hughes (*Rutgers University*)

P. Hardee (*University of Alabama*)

HEAD/APS Meeting, April 20 - 23, 2002

1. Motivations

- **Accretion disk dynamics including azimuthal instabilities such as magnetorotational instability (MRI) and *accretion-disk instabilities* with various initial and magnetic field geometries**
- **Variabilities of relativistic jets due to the instabilities in the accretion disk and their effects on jet propagations**
- **Calculate iron emission line from the inner region of accretion disk around a black hole comparing with observations**
- **Examination of Blandford-Znajek model with a Kerr black hole as a possible energy source for Gamma-ray Bursts?**

Scientific objectives

- **How do accretion disks near black holes evolve under the influence of accretion-disk instabilities?**
- **How do these instabilities affect associated jet formation?**
- **How do our full 3-D GRMHD simulations with a Kerr black hole support Blandford-Znajek model?**
- **What is the main mechanism of relativistic jet formation?**
- **How is the relativistic jet collimated in the process of its formation?**
- **How do relativistic jets propagate?**

2. Theoretical models of jet formation

Lovelace (1976), Blandford (1976)

Blandford &Znajek (1997): Kerr black hole

Blandford and Payne (1982):

Magneto-centrifugal force-driven jet

Begeleman, Blandford, & Rees (1984):

"Theory of extragalactic radio sources"

Uchida & Shibata (1985): Magnetically driven

Koide, Shibata & Kudoh (1998): (2-D GRMHD)

"*Gas pressure*" & Magnetically driven

3. Simulation models

- General relativistic MHD codes

  axisymmetric (2-D) and full 3-D models

  Schwarzschild and Kerr black holes

  with simplified Total Variation Diminishing (TVD) method (Davis 1984)

  (Lax-Wendroff's method with additonal diffusion term)

Fundamental equations

- $\nabla_\nu (\rho U^\nu) = 0$ (**Conservation of mass**)
- $\nabla_\nu T_g^{\mu\nu} = 0$ (**Conservation of momentum**)
- $\partial_\mu F_{\nu\lambda} + \partial_\nu F_{\lambda\mu} + \partial_\lambda F_{\mu\nu} = 0$

  (**Conservation of energy for single component conductive fluid**)
- $\nabla_\mu F^{\mu\nu} = - J^\nu$ (**Maxwell's equations**)

  $F_{\mu\nu}$ **(electromagnetic field-strength tensor)**

  $F_{\mu\nu} = \partial_\mu A_\nu - \partial_\nu A_\mu$

  $F_{\nu\mu} U^\nu = 0$ (**Frozen-in condition**)

$\boldsymbol{U}^{\nu}$: velocity 4-vector

$\boldsymbol{J}^{\nu}$: current 4-vector

ρ : proper mass density

p : proper pressure

$e = \rho c^2 + p/(\Gamma - 1)$: energy density

Γ: specific-heat ratio (5/3)

∇_{μ} : covariant derivative

$\boldsymbol{T}_{\mathrm{g}}{}^{\mu\nu} = pg^{\mu\nu} + (e+p)\boldsymbol{U}^{\mu}\boldsymbol{U}^{\nu} + \boldsymbol{F}^{\mu\sigma}\boldsymbol{F}^{\nu\sigma} - g^{\mu\nu}\boldsymbol{F}^{\lambda\kappa}\boldsymbol{F}_{\lambda\kappa}/4$:

general relativistic energy momentum tensor

$\boldsymbol{A}^{\mu}$: potential 4-vector

3+1 Formalism of General Relativistic MHD Equations

$$\partial D/\partial t = -\nabla\cdot(D\boldsymbol{v})$$

$$\partial \boldsymbol{P}/\partial t = -\nabla\cdot[p\boldsymbol{I}+\gamma^2(e+p)\boldsymbol{vv}/c^2-\boldsymbol{BB}-\boldsymbol{EE}/c^2+0.5*(B^2+E^2/c^2)\boldsymbol{I}]$$

$$\partial \epsilon/\partial \mathrm{t} = -\nabla\cdot[\{\gamma^2(e+p)-D^2c^2\}\boldsymbol{v}+\boldsymbol{E}\times\boldsymbol{B}]$$

$$\partial \boldsymbol{B}/\partial t = -\nabla\times\boldsymbol{E}$$

$$(1/c^2)\partial \boldsymbol{E}/\partial t + \boldsymbol{J} = -\nabla\times\boldsymbol{B}$$

$$(1/c^2)\,\nabla\cdot\boldsymbol{E} = \rho_c$$

$\boldsymbol{E} = -\boldsymbol{v}\times\boldsymbol{B}$ (Frozen-in condition)

$\gamma \equiv [1-(v/c)^2]^{-1/2}$, $D = \gamma\rho$, $\boldsymbol{P} = \gamma^2(e+p)\boldsymbol{v}/\mathrm{c}^2 + \boldsymbol{E}\times\boldsymbol{B}/\mathrm{c}^2$

$$\epsilon = \gamma^2(e+p)-p-Dc^2+0.5*(B^2+E^2/\mathrm{c}^2)$$

Metric and Coordinates

Schwarzschild metric: $ds^2 = g_{\mu\nu} dx^\mu dx^\nu$

Boyer-Lindquist set (ct, r, θ, ϕ)

Off-diagonal elements of metric are zero

$$g_{\mu\nu} = 0 \quad (\mu \neq \nu)$$

$$g_{00} = -h_0^2, \; g_{11} = h_1^2, \; g_{22} = h_2^2, \; g_{33} = h_3^2$$

$$h_0 = \alpha, \; h_1 = 1/\alpha, \; h_2 = r, \; h_3 = r \cos\theta$$

$$\alpha \equiv (1 - r_S / r)^{1/2} \quad \text{(lapse function)}$$

Tortoise Coordinates

$d/dr_* \equiv (r - r_S)d/dr$ $\quad$ $r_* = \ln(r - r_S)$

Schwarzschild radius: $r_S \equiv 2GM_{BH}/c^2$

Time Constant: $\tau_S \equiv r_S/c$

Boundary conditions at r = 1.1, 20 r_S: radiating

CFL numerical stability condition is severe at r =1.5 r_S

Polytropic equation of state: $p = \rho^\Gamma$

Γ =5/3 and H = 1.3

Initial conditions

•Free-falling corona (these simulations)

accretion disk

relativistic Keplerian velocity $v_\phi = v_K \equiv c/[2(r/r_S - 1)]^{1/2}$

$\rho = \rho_{ffc} + \rho_{dis}$ $\qquad r_D \equiv 3\, r_S$

$$\rho_{dis} = \begin{cases} 100\, \rho_{ffc} & \text{if } r > r_D \text{ and } |\cot\theta| < \delta \\ 0 & \text{if } r \le r_D \text{ or } |\cot\theta| \ge \delta \end{cases} \qquad (\delta = 0.125)$$

$$(v_r, v_\theta, v_\phi) = \begin{cases} (0, 0, v_K) & \text{if } r > r_D \text{ and } |\cot\theta| < \delta \\ (-v_{ffc}, 0, 0) & \text{if } r \le r_D \text{ or } |\cot\theta| \ge \delta \end{cases}$$

Simulation parameters

$1.1r_S \le r \le 20r_S$, $0 \le \theta \le \pi$, $0 \le \phi \le 2\pi$

(r, θ, ϕ) : $200 \times 70 \times 2$ (2D), **100 ´ 60 ´ 120 grids (3D),**

$B_0 = 0.3(\rho_0 c^2)^{1/2}$, $B_r = B_0 \cos\theta$, $B_\theta = -\alpha B_0 \sin\theta$

$H = \alpha\gamma h/\rho c^2$ (specific enthalpy)

$h \equiv \rho c^2 + \Gamma p(\Gamma - 1)$ (relativistic enthalpy)

$Q \equiv \rho\gamma u$ (mass) , $P \equiv hu^2 + p$ (total pressure)

$v_s \equiv (\Gamma p/h)^{1/2} c$ (sound velocity), $u \equiv \gamma v/c$

$\beta \equiv p/B^2 = 1.40$ (at $r = 3r_S$) (Plasma beta)

$v_A \equiv cB(\rho + [\Gamma p(\Gamma - 1) + B^2)]\,)^{-1/2} = 0.015c$, (Alfven velocity (FIDO))

2-D axisymmetric simulation

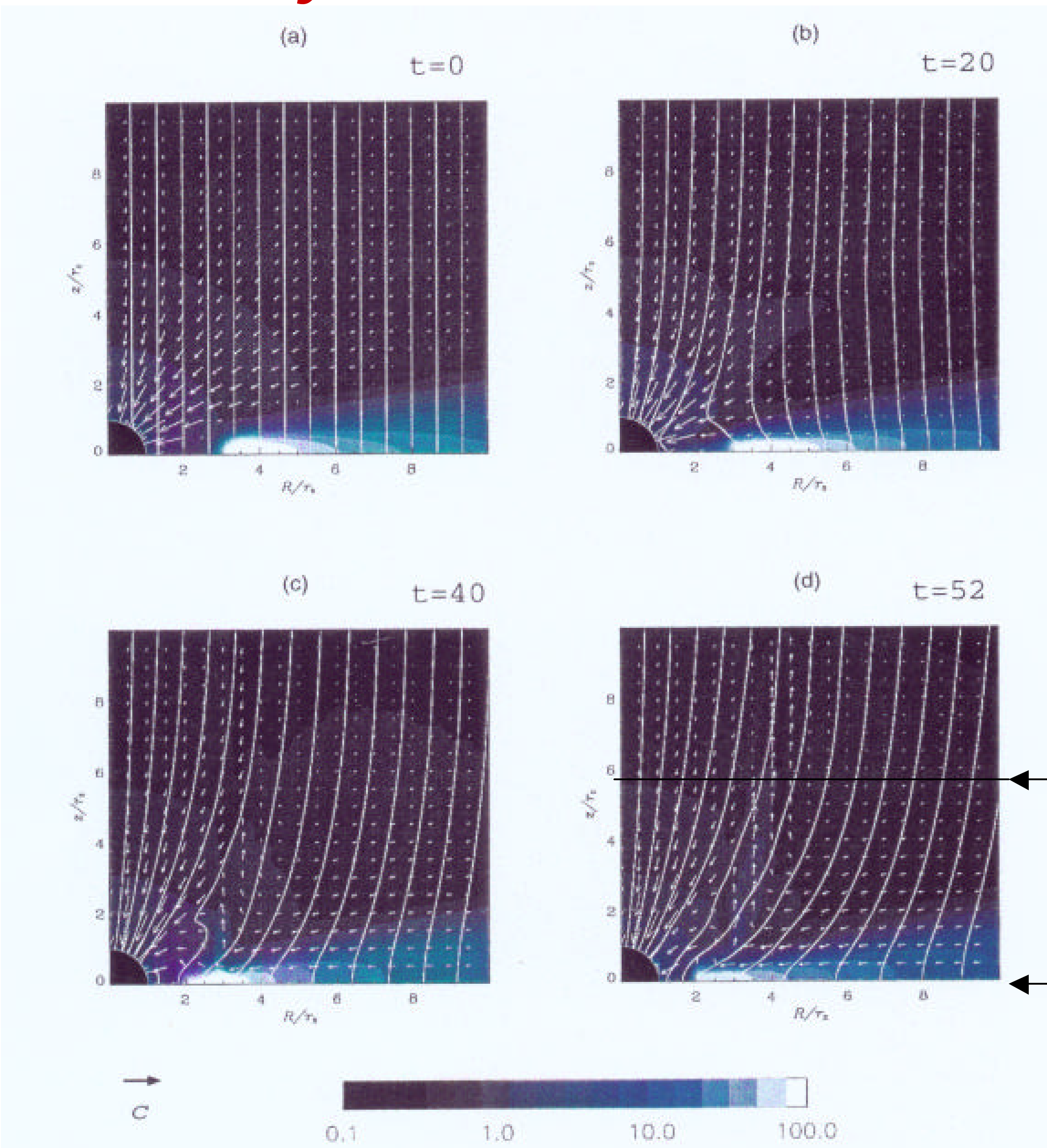

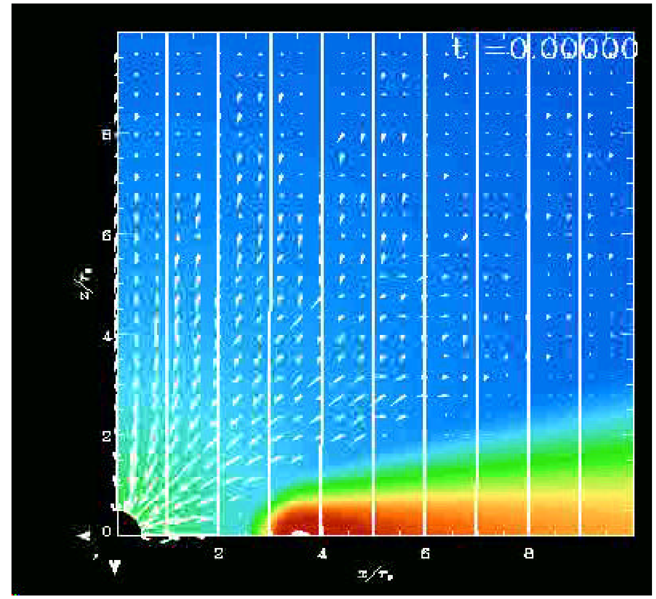

Movie

$z = 5.6\ r_s$

$z = 0.0 r_s$

(Koide et al. 1999)

Radial Profiles, equatorial plane (z = 0), t=52 τ_S

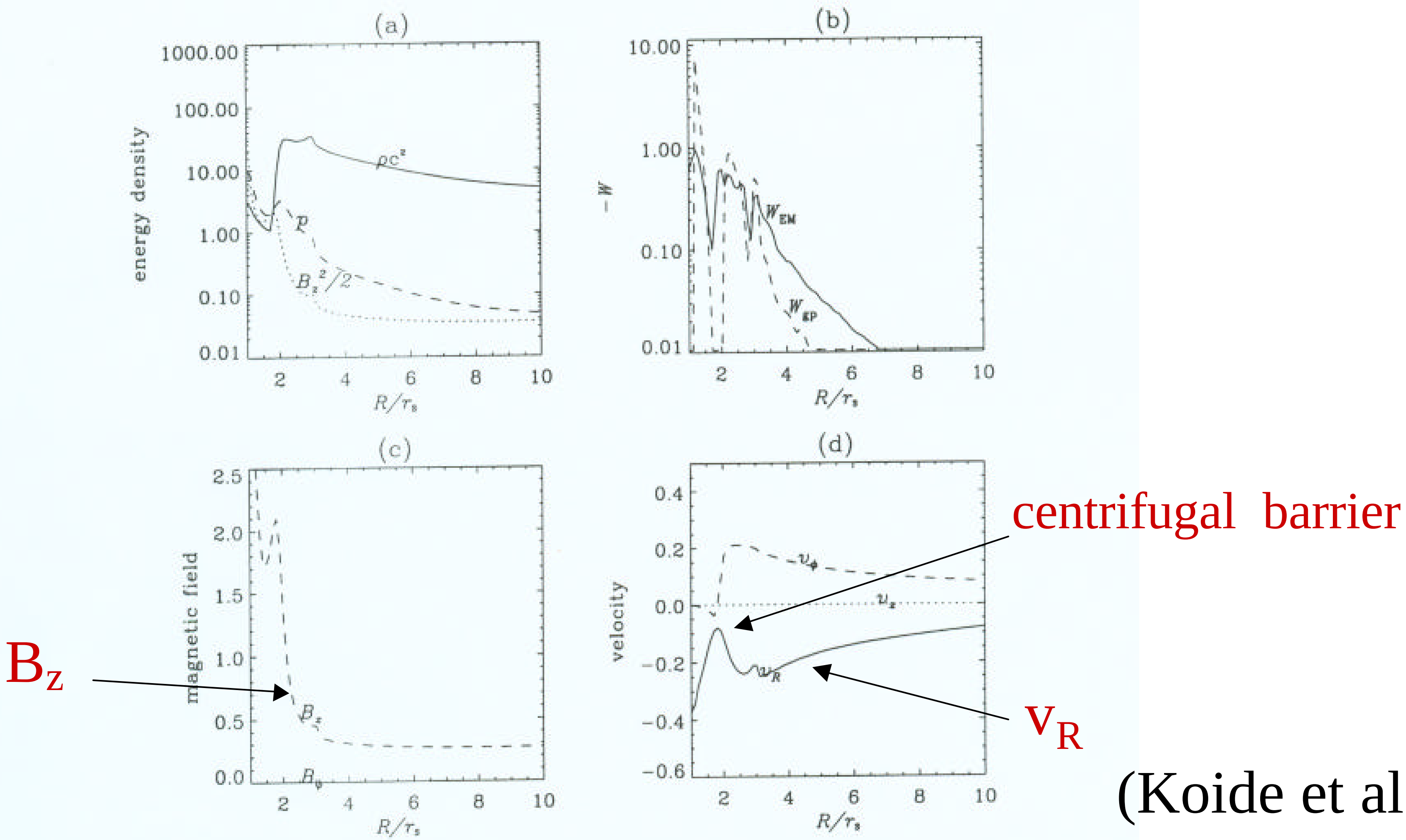

FIG. 7.—Various physical quantities on the equatorial plane, $z = 0$ at $t = 52\tau_S$, in the free-fall (steady state falling) corona case. (*a*) Proper mass density ρ (*solid line*), proper pressure p (*dashed line*), and magnetic field energy $B_z^2/2$ (*dotted line*). (*b*) The power contribution of the gas pressure, W_{gp} (*dashed line*), and the electromagnetic force, W_{EM} (*solid line*), to evaluate the deceleration effect of the accreting disk plasma. (*c*) The components of the magnetic field, B_ϕ and B_z. (*d*) The components of the velocity, v_R, v_z, and v_ϕ. We can see the shock front at $r = 3r_S$.

(Koide et al. 1999)

Radial Profiles, (z = 5.6 r_s), t=52 τ_S

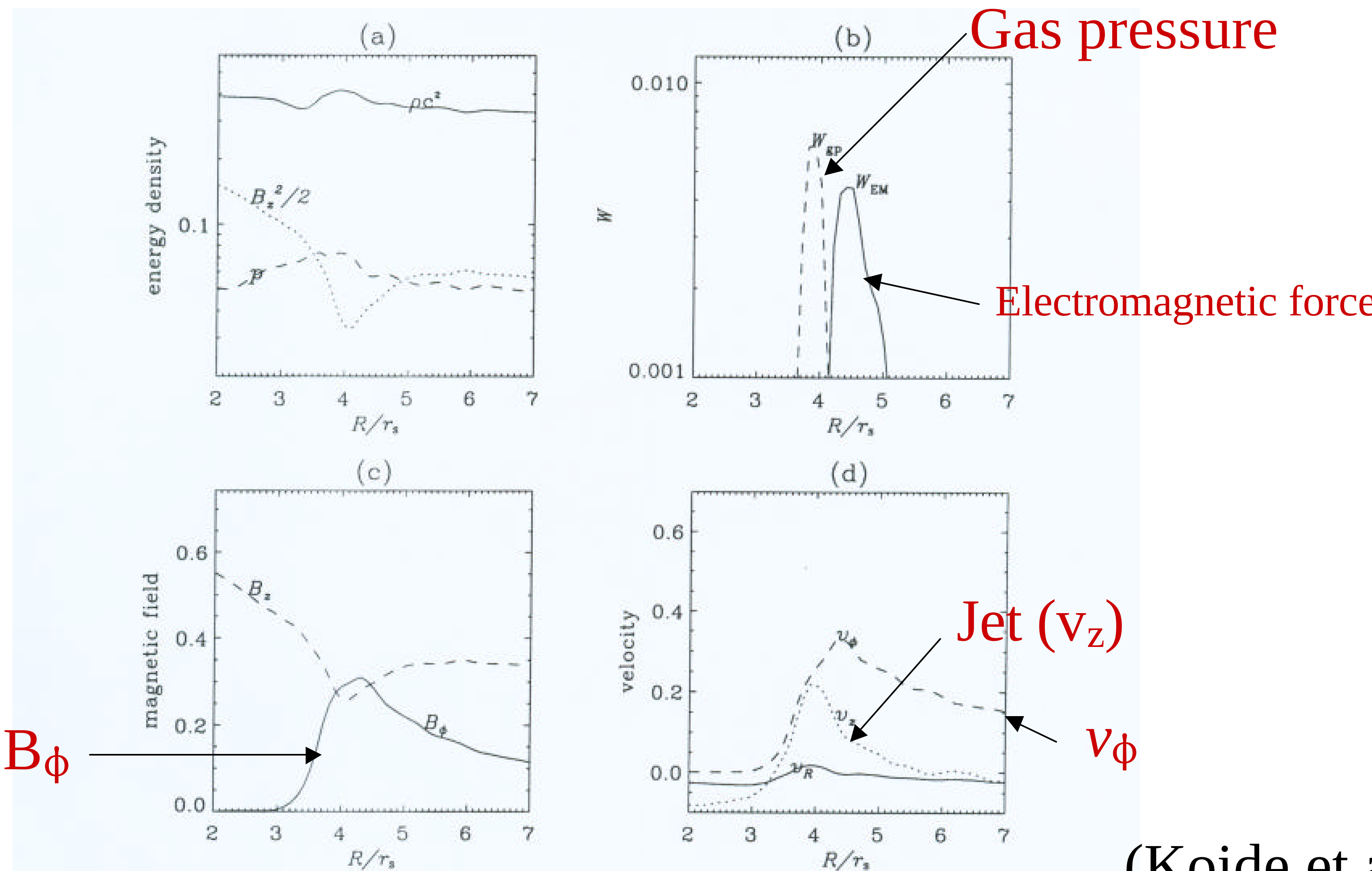

FIG. 8.—Various physical quantities on the $z = 5.6r_s$ surface at $t = 52\tau_s$ in the free-fall (steady state falling) corona case. (*a*) Proper mass density ρ (*solid line*), proper pressure p (*dashed line*), and magnetic field energy $B_z^2/2$ (*dotted line*). The jet is located around $R = 3.8r_s$. (*b*) The power contribution of the gas pressure, W_{gp} (*dashed line*), and the electromagnetic force, W_{EM} (*solid line*), to evaluate the acceleration of the jet. We can clearly see the two-layer acceleration region in the jet. (*c*) The components of the magnetic field, B_ϕ and B_z. (*d*) The components of the velocity, v_R, v_z, and v_ϕ. The jet spreads through $3r_s \le R \le 5r_s$.

(Koide et al. 1999)

3-D simulation   mass density ($\log_{10} \rho$)

$t = 0.0\ \tau_S$ **$t = 39.2\tau_S$**

Accretion disk

$t = 60.0\tau_S$ **$t = 73.9\tau_S$**

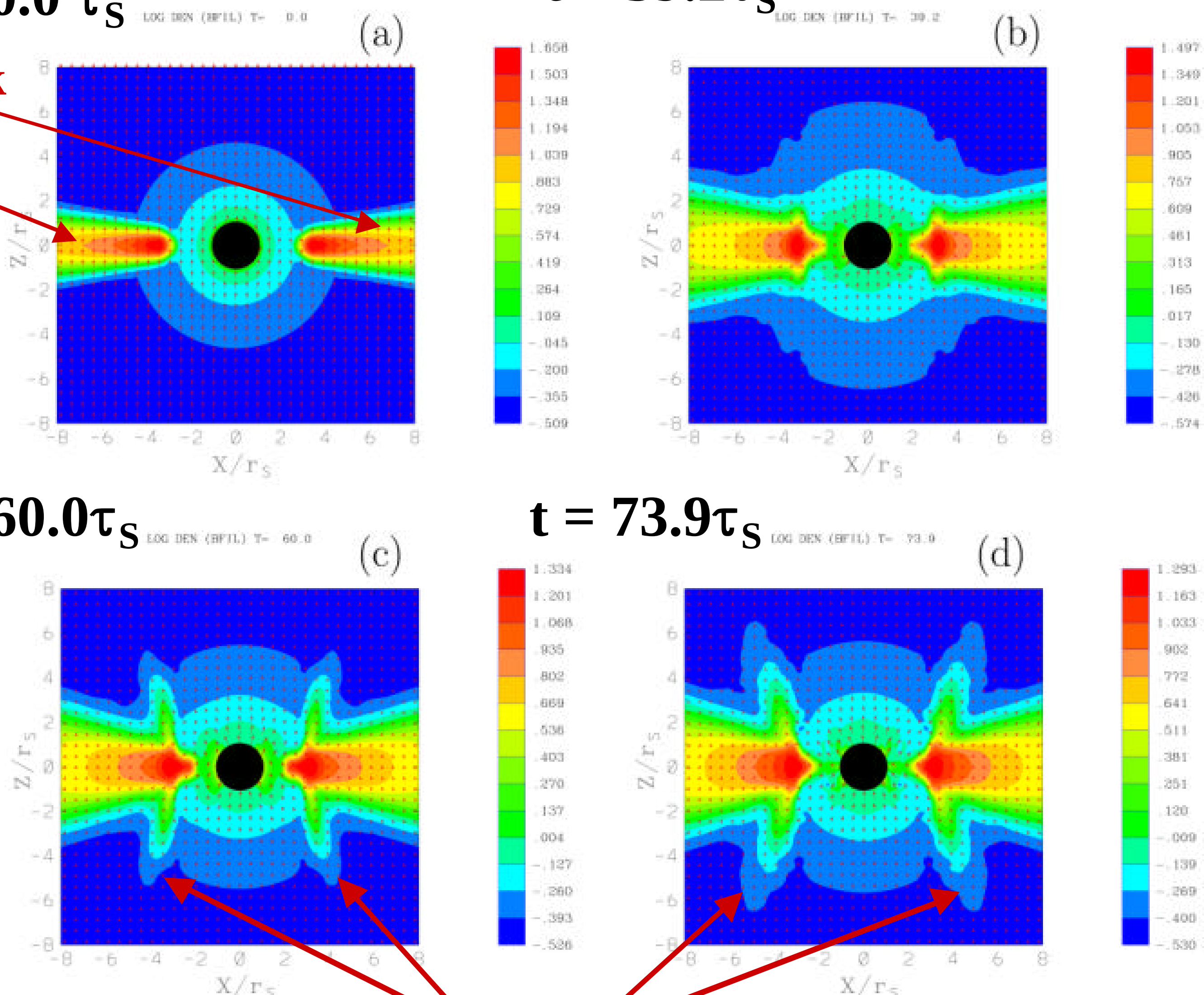

● Black hole   **Jet**

Nishikawa et al (2002)

Pressure ($\log_{10}$ p)

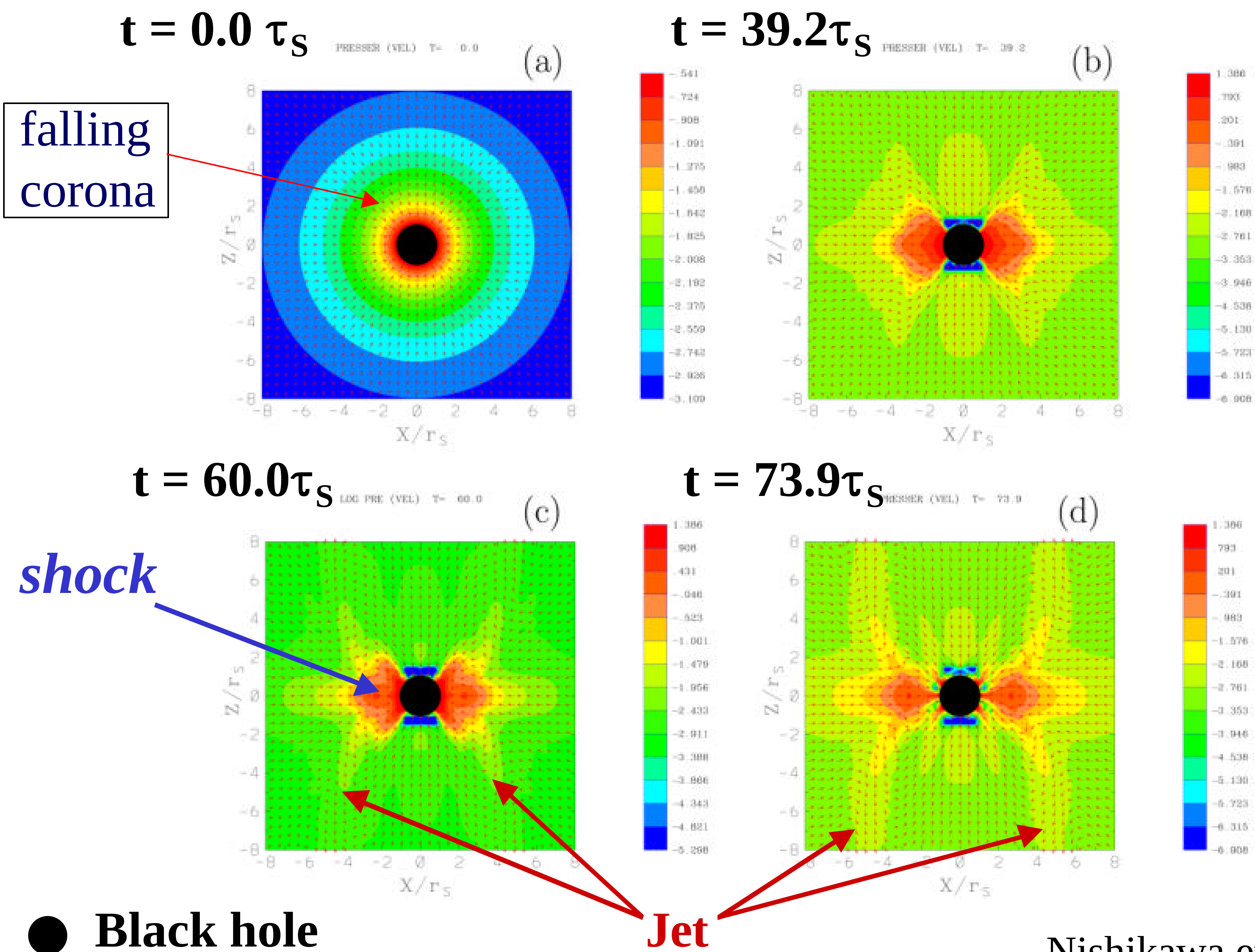

Nishikawa et al (2002)

Twisted magnetic fields by accretion disk

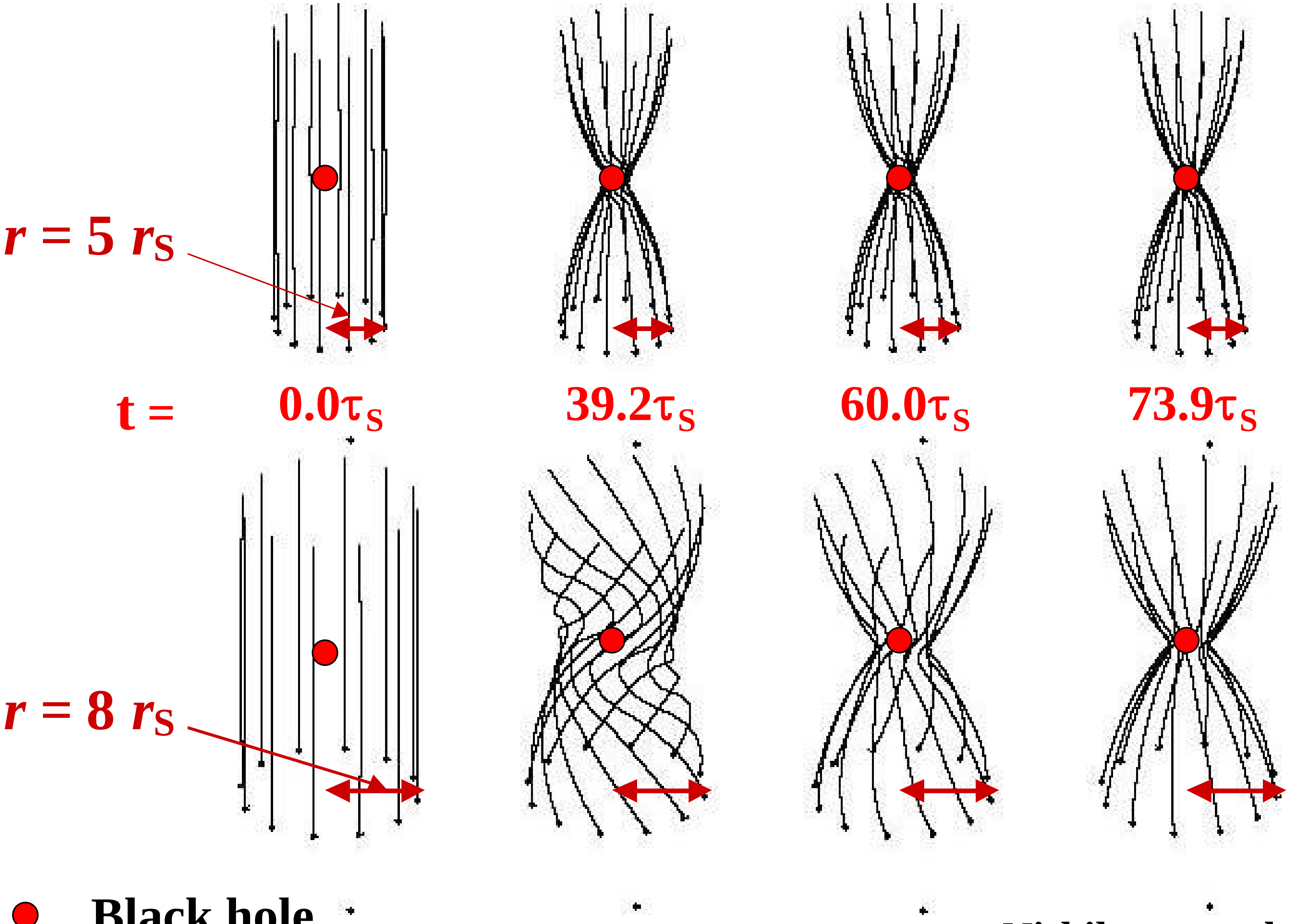

Nishikawa et al (2002)

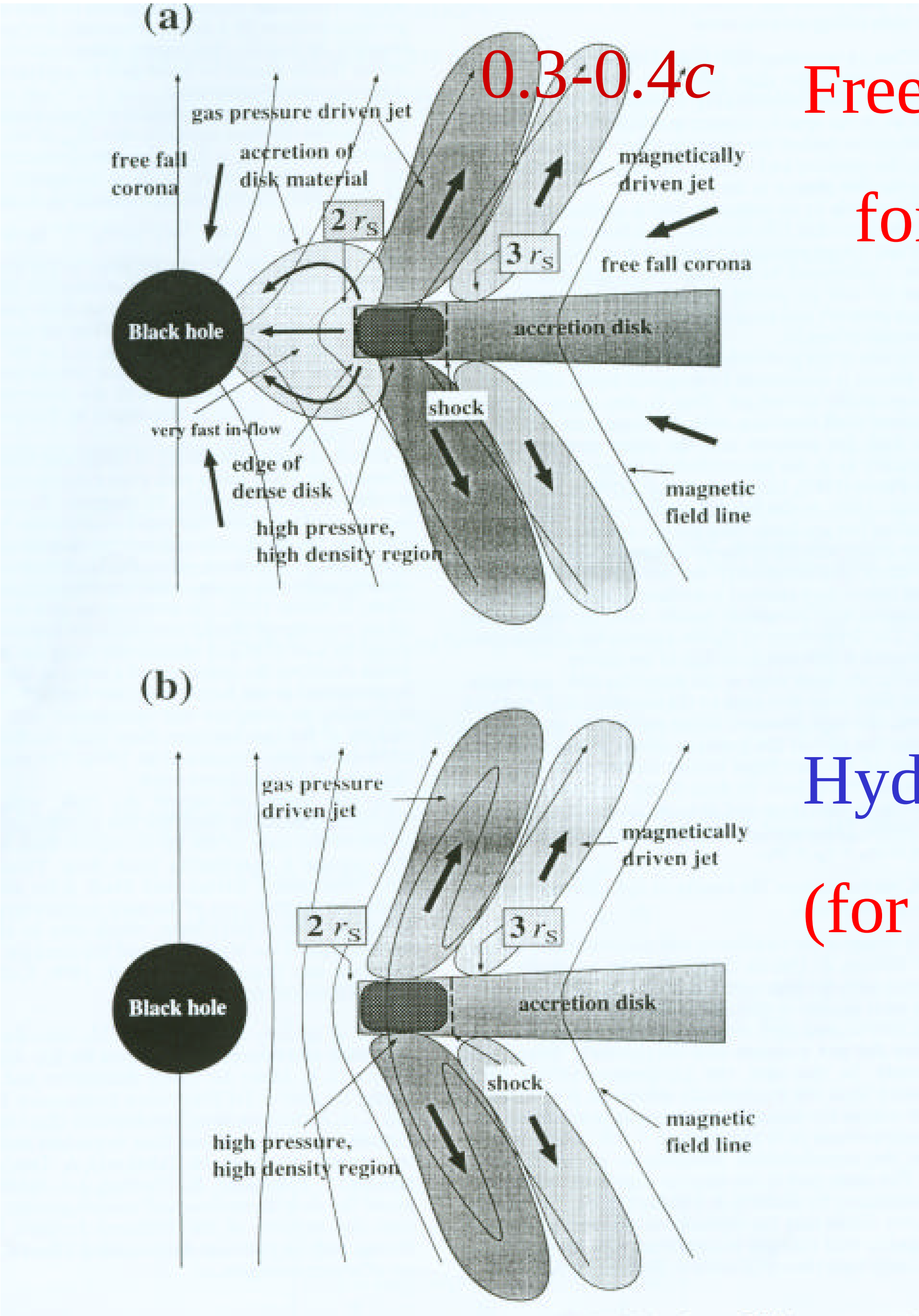

Free-falling corona

for black holes

Schematic picture of two-layer shell structure of relativistic jet

Hydrostatic equilibrium corona

(for protostellar objects)

(Koide et al. 1999)

Summary

- Comparing the axisymmetric (2-D) simulations 3-D simulation show slower growth of jet formation
- The additional freedom in the azimuthal direction without the mirror symmetry at the equatorial plane slows down the pill-up due to shocks near the black hole
- In order to see effects of instabilities we need to seed initial perturbations with accretion disks

Future Plans for jet formation study

- **Investigation of jet generation from Schwarzschild and Kerr black holes using full 3-D GRMHD simulations with better resolutions and for a long time**
- **Change initial conditions including magnetic field geometries and accreting stream from mass donor stars to examine how the accretion disk dynamics and associated jet formation depend on initial conditions**
- **Improve 3-D displays in order to understand physics involved in simulations**
- **Implement a better boundary condition at the horizon**
- **Investigate iron line emission from the inner accretion disk near black holes compared with observations by Chandra, BATSE, XMM, ASTRO E2, GLAST, and Constellation-X**
- **Investigate the dynamics of Kerr black hole as an energy source for Gamma-ray bursts**